



HAL
open science

Assessment of a wave-forced Richards' equation-based model regarding beach groundwater flow experiments

Jean-Baptiste Clément, Damien Sous

► **To cite this version:**

Jean-Baptiste Clément, Damien Sous. Assessment of a wave-forced Richards' equation-based model regarding beach groundwater flow experiments. *Experimental Fluid Mechanics* 2022, Nov 2022, Dvůr Králové nad Labem, Czech Republic. hal-03937176

HAL Id: hal-03937176

<https://hal.science/hal-03937176>

Submitted on 13 Jan 2023

HAL is a multi-disciplinary open access archive for the deposit and dissemination of scientific research documents, whether they are published or not. The documents may come from teaching and research institutions in France or abroad, or from public or private research centers.

L'archive ouverte pluridisciplinaire **HAL**, est destinée au dépôt et à la diffusion de documents scientifiques de niveau recherche, publiés ou non, émanant des établissements d'enseignement et de recherche français ou étrangers, des laboratoires publics ou privés.

Assessment of a wave-forced Richards' equation-based model regarding beach groundwater flow experiments

Jean-Baptiste Clément^{1*}, and Damien Sous^{2,3}

¹Department of Technical Mathematics, Faculty of Mechanical Engineering, Czech Technical University in Prague, Prague, Czechia

²Mediterranean Institute of Oceanography (MIO), Université de Toulon, Aix-Marseille Université, La Garde, France

³SIAME, Université de Pau et des Pays de l'Adour (UPPA), Anglet, France

Abstract. A numerical model is proposed to analyse the effect of waves in near-shore waters on the beach groundwater flow. The groundwater flow is modelled by Richards' equation which describes flows in variably-saturated porous media. A wave-driven boundary conditions is prescribed at the beach face. The model abilities are assessed against the results of a large-scale laboratory experiment called BARDEX II. This is a sand barrier with a lagoon whose level is controlled. The investigation of water flow rates through the barrier highlights the beach groundwater dynamics under different conditions.

1 Introduction

Around one-third of the world's ice-free coastline are sandy beaches. Satellite data analysis indicates that a quarter of them are under erosion. There is a serious concern about their future evolution.

Beach groundwater dynamics has become a topic of interest over the years because it controls many processes like biogeochemical cycles, sediment transport, contaminant exchanges, *etc.* The beach groundwater is mainly governed by the cross-beach gradients induced by tides or large-scale fluctuations of mean water level such as swell and infragravity waves [1]. The swash zone is the beach part subject to waves action. The interaction of the sheet of water with the porous beach causes infiltrations/exfiltrations through the beach face. They can in turn affect the beach groundwater dynamics, especially the unsaturated part.

Although significant understanding of swash groundwater dynamics has been gained, experiments are limited because they are heavy to deploy, instruments lack spatio-temporal resolutions and measurements are quite intrusive [1,2]. Then, numerical models are needed to complete experimental insights. Even though extensive modelling effort has been provided over the last two decades, the proposed models [3,4-6] are mostly based on Darcy's theory or horizontal dynamics (Dupuit-Forchheimer assumption). Thus, their scope remains limited since they ignore partial saturation and capillarity effect which are essential in fine-grained sand beaches. Indeed, field experiments demonstrated the presence of a circulation cell with vertical head gradients in sandy beaches [1]. To tackle these issues, the present study aims to model wave-resolved variably-saturated groundwater flow based on Richards'

equation. Up to now, there are very few attempts to implement wave-forced Richards' equation [7].

The simulation of swash beach groundwater is challenging because the problem holds a wide range of space/time scales. Indeed, on one hand, waves have fast dynamics while groundwater is slow and on the other hand, swash infiltrations/exfiltrations have local effects while cross-beach gradients affect the whole beach. A numerical strategy has been developed in [8] to solve efficiently Richards' equation. The resulting code, called *Rivage*, is used in this study to simulate wave-resolved beach groundwater dynamics.

The first section deals with the model problem based on Richards' equation. Then, a brief description of the numerical methods used to solve Richards' equation is presented. The next section is dedicated to the results. A comparison is made with BARDEX II experiments. Finally, some conclusive remarks are given.

2 Model problem

The modelling of wave-forced groundwater flows in unsaturated porous media is introduced.

2.1 Richards' equation

Richards' equation is a non-linear degenerate parabolic equation to describe flows in variably-saturated porous media. Both the saturated and unsaturated zones are modelled. Yet, Richards' equation considers only the water phase which makes it competitive to simulate compared to full two-phase flow models. Richards' equation is based on the assumption that air phase is continuously-connected with the atmosphere and neglects inertial effects.

* Corresponding author: jean-baptiste.clement@fs.cvut.cz

The Richards' equation under mixed formulation [9] is written in terms of hydraulic head $h = \psi + z$ [L]:

$$\partial_t \theta(h - z) - \nabla \cdot (\mathbf{K}(h - z) \nabla h) = 0, \quad (1)$$

where ψ is the pressure head [L], θ the water content [-], \mathbf{K} the hydraulic conductivity [$L \cdot T^{-1}$] and z the elevation [L]. The saturated ($\psi \geq 0$) and unsaturated ($\psi < 0$) zones are separated by the water table ($\psi = 0$). The capillary fringe is the unsaturated part almost entirely filled by water, just above the water table.

Richards' equation needs two constitutive laws to be solved: one for the water content and one for the hydraulic conductivity. The water content is described in terms of effective saturation S_e [-] and the tensor of hydraulic conductivity is supposed to react to pressure head identically for each space direction:

$$\theta(\psi) = \theta_s + (\theta_s - \theta_r) S_e(\psi), \quad (2)$$

$$\mathbf{K}(\psi) = \mathbf{K}_s K_r(\psi), \quad (3)$$

where θ_s is the saturated water content [-], θ_r the residual water content [-], \mathbf{K}_s is the saturated hydraulic conductivity tensor [$L \cdot T^{-1}$] and K_r the relative hydraulic conductivity [-]. These two hydraulic properties have two different behaviours which explains the degeneracies of Richards' equation:

$$S_e(\psi) = \begin{cases} 1 & \text{if } \psi \geq 0, \\ S_e^*(\psi) & \text{otherwise,} \end{cases} \quad (4)$$

$$K_r(\psi) = \begin{cases} 1 & \text{if } \psi \geq 0, \\ K_r^*(\psi) & \text{otherwise.} \end{cases} \quad (5)$$

S_e^* and K_r^* are monotonic increasing functions of pressure head in the unsaturated zone. In this paper, the Van Genuchten-Mualem relations [10,11] are used:

$$S_e^*(\psi) = (1 + (\alpha|\psi|^n)^{-m}), \quad (6)$$

$$K_r^*(\psi) = S_e^{*0.5}(\psi) (1 - (1 - S_e^{*1/m}(\psi))^m)^2, \quad (7)$$

where α denotes a parameter [L^{-1}] linked to air entry pressure inverse, $n > 1$ a pore-size distribution parameter [-] and $m = 1 - \frac{1}{n}$ [-].

2.2 Wave-driven boundary conditions

Classical boundary conditions can be applied to Richards' equation: a Dirichlet boundary condition enforces the hydraulic head and a Neumann boundary condition enforces the flux.

In addition, a specific boundary condition, called seepage, can be used for Richards' equation to model the interaction of porous media flow with atmosphere. This seepage boundary condition works as an outflow condition. If the porous medium is saturated, then the water pours out at atmospheric pressure. If the porous medium is unsaturated, then the water is prevented to go out. This condition can be written under many formulations but it can be viewed as a switch between a Dirichlet (prescribed zero pressure head) and a Neumann (prescribed zero flux) boundary conditions

according to the state of saturations of the porous medium. Then, seepage can be interpreted as a nonlinear Robin boundary condition. For this study, the seepage boundary condition is treated inside the nonlinear iterative scheme according to the previous solution guess at a local level of the numerical scheme, as described in Clément *et al.* [8]. This technique needs no restrictive *a priori* assumption on the seepage face.

In order to take into account the waves, a dynamic boundary condition is built to force the Richards' equation. It combines a Dirichlet and a seepage boundary condition. The former applies the hydraulic head induced by the water column wherever the swash tongue floods the beach. The latter is applied to the remaining part of the beach, beyond the swash tip. Thereby, the waves forcing condition allows the swash tip and the water table to be disconnected.

The surface water is computed by the open-source SWASH code which solves the nonlinear shallow water equations including non-hydrostatic pressure [12]. All parameters being kept by default, this wave-resolving model is used to get the bottom pressure which serves to monitor the Dirichlet boundary condition in space and time. From a technical point of view, the SWASH data are adapted to the groundwater model by performing linear interpolation of the space-time grids. The position of the swash tip is also provided to make explicitly the switch between the Dirichlet and seepage boundary conditions.

3 Numerical methods

Even though Richards' equation is widely used in the hydrogeology field, it remains challenging to solve. Indeed, due to the behaviour of hydraulic properties, nonlinear convergence is difficult to achieve and can even fail [9]. In addition, the solution of Richards' equation is known to exhibit spurious oscillations because of the degeneracies. Typically, an undershoot can appear ahead of a sharp wetting front propagating into an initially dry soil. These drawbacks make Richards' equation costly to compute [9]. In the case of wave-driven problems, the simulation of successive rapidly-varying infiltrations is demanding. Thus, a numerical strategy has been developed to alleviate these issues in Clément *et al.* [8]. The main tools are presented briefly hereinafter.

Space discretization of Richards' equation (1) is done by a discontinuous Galerkin (DG) method called IIPG (Incomplete Interior Penalty Galerkin) because this formulation remains simple. Extensive introduction of DG methods can be found in the Rivière's textbook [13]. The implicit Euler scheme is used for time discretization because it shows a wide region of stability needed for the Richards' equation known to be stiff. Linearization is achieved through a fixed-point method. It is linearly convergent while Newton-Raphson method is quadratically convergent but the former is more robust since it is not sensitive to the initial guess. In addition, an adaptive strategy based on a weighted DG framework and local mesh refinement is used to help with the solving of Richards' equation, see [8].

4 Results

The wave-forced Richards' equation-based model is used to assess water flow rates through an experimental beach barrier under different conditions.

4.1 Experimental and numerical set-ups

The BARDEX II project is a set of large-scale experiments conducted in July 2012 at the Delta Flume in the Netherlands [1,14]. They focus on the groundwater dynamics in a sand barrier under controlled laboratory conditions. Figure 1 represents the experimental set-up. The sand barrier is 4.5 m high and 5 m wide. The barrier profile has five sections: (i) a concrete toe of slope 1:10 ($24 < X < 29$ m), (ii) a horizontal section ($29 < X < 49$ m), (iii) a beach face of seaward slope of 1:15 ($49 < X < 109$ m), (iv) a horizontal crest of height 4.5 m ($109 < X < 114$ m) and (v) a landward slope of 1:5 ($114 < X < 124$ m). A permeable retaining wall separates the barrier from a 10 m long lagoon.

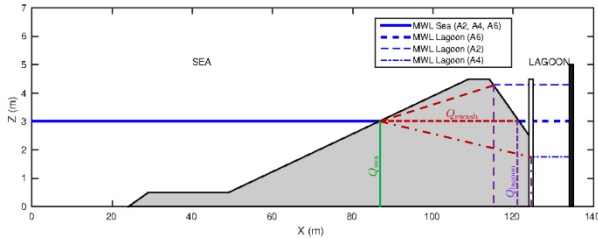


Fig. 1. Description of the experimental set-up for the BARDEX II cases. The mean water level (MWL) at sea constant while the lagoon MWL can be kept higher (A2), lower (A4) or same (A6) level. The green/red/violet lines indicate respectively the sea/swash/lagoon control planes for the water flow rate.

Six experimental cases are selected to assess the effects of waves and cross-barrier gradients on the groundwater dynamics. Parameters are compiled in Table 1 where H_s is the significant wave height and T_p is the peak period. Each case is a run of 300 s.

Table 1. BARDEX II experimental cases.

Case	H_s (m)	T_p (s)	MWL sea (m)	MWL lagoon (m)
A2	-	-	3	4.3
A2w	0.8	8	3	4.3
A4	-	-	3	1.75
A4w	0.8	8	3	1.75
A6	-	-	3	3
A6w	0.8	8	3	3

The barrier sand has been characterized in [2]. In the present study, the relations (6) and (7) are used with hydraulic parameters from a similar sand found in [15] (Vail sand): $\alpha = 4.6 \text{ m}^{-1}$, $n = 5.14$, $\theta_s = 0.41$, $\theta_r = 0.03$ and $K_s = 8 \times 10^{-4} \text{ m} \cdot \text{s}^{-1}$. The SWASH model provides the free surface forcing on the beach face. The remaining boundary conditions for the simulation are similar as described in [3]. Initialization of groundwater

is done in a such a way to match the initial state reached by the experimental runs described in [14].

4.2 Comparison of water flow rates through the barrier

From BARDEX II experiments, Turner *et al.* [14] calculated the averaged cross-barrier fluxes at the vertical cross-sections near the sea and the lagoon, as shown in Figure 1. These horizontal averaged flow rates were also computed from the numerical simulations of the Richards' equation-based model. The results are summarised in Table 2. Experimental and numerical values differ within a factor 2-3 which is reasonable in the field of hydrogeology [14] and supports the numerical estimates from the present model. Besides, one should note that experimental results only account for flows in the saturated part unlike the numerical model. When there is no wave, horizontal fluxes are driven by the gradients induced by the difference of sea and lagoon level. For the case A6, experimental fluxes are not negligible which indicates that the steady state was not reached as expected. Under waves action, the horizontal flux at sea is increased and it is seaward irrespective to the lagoon level. It shows that infiltration induced by waves are powerful enough to drive flows in the lower part of the swash zone.

Table 2. Averaged flow rates through the sea/lagoon vertical control planes shown in Figure 1. Positive/negative flow rates are respectively landward/seaward. Experimental results from [14] are in blue and numerical results are in red.

Case	Sea control plane ($\text{m}^3 \cdot \text{s}^{-1}$)	Lagoon control plane ($\text{m}^3 \cdot \text{s}^{-1}$)
A2	-2.05×10^{-4} -4.91×10^{-4}	-3.75×10^{-4} -6.06×10^{-4}
A4	8.70×10^{-5} 3.37×10^{-4}	6.46×10^{-5} 3.13×10^{-4}
A6	-9.38×10^{-5} -2.14×10^{-15}	-1.74×10^{-5} 1.61×10^{-15}
A2w	-3.14×10^{-4} -4.89×10^{-4}	-2.58×10^{-4} -4.82×10^{-4}
A4w	-3.83×10^{-4} -5.28×10^{-4}	7.55×10^{-5} 4.72×10^{-4}
A6w	-4.45×10^{-4} -7.08×10^{-4}	4.78×10^{-5} 2.08×10^{-4}

In order to assess the effect of waves in the swash zone, the numerical simulations are used to compute normal fluxes through a control plane linking and closing the upper part of the sea and lagoon cross-sections, as shown in Figure 1. Results are presented in the Table 3. Indeed, they show infiltrations are increased with waves action.

Table 3. Averaged flow rates through the swash control planes shown in red in Figure 1 from the numerical results. Negative flow rates are inflows.

Case	Swash control plane ($\text{m}^3 \cdot \text{s}^{-1}$)	Case	Swash control plane ($\text{m}^3 \cdot \text{s}^{-1}$)
A2	-1.79×10^{-3}	A2w	-2.32×10^{-5}
A4	-6.64×10^{-6}	A4w	-1.02×10^{-3}
A6	-7.73×10^{-15}	A6w	-9.03×10^{-4}

Figures 2, 3 and 4 bring insights about the repartition of averaged inflow/outflow in the upper part of the barrier under waves action. They confirm that the lagoon has limited influence. However, waves establish over time a circulation cell with infiltration/exfiltration respectively in the upper/lower part of the swash zone, which supports experimental observations [1,14]. For the cases A4w and A6w, infiltrations are important enough to explain the seaward horizontal flux. For the case A2w, infiltration is not dominant but the high lagoon level explains then the seaward horizontal flux.

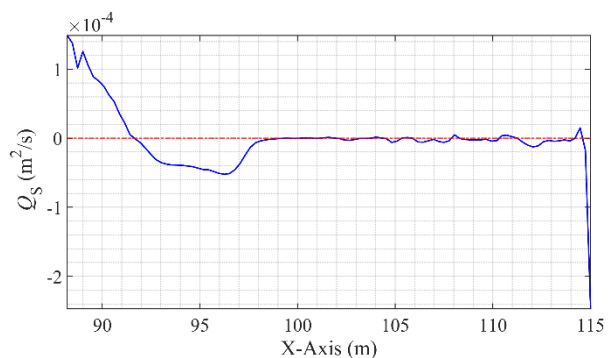


Fig. 2. Averaged surface flow rate (normal) along the swash control plane in the case A2w (sea level < lagoon level) from numerical results.

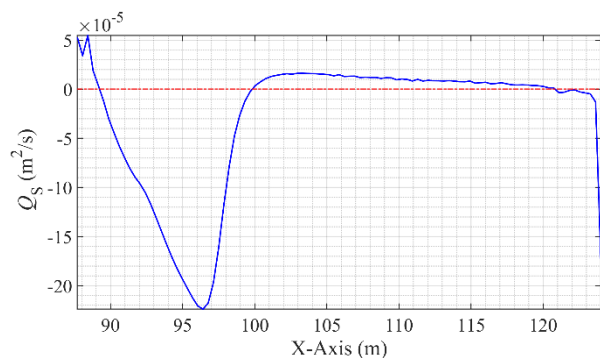


Fig. 3. Averaged surface flow rate (normal) along the swash control plane in the case A4w (sea level > lagoon level) from numerical results.

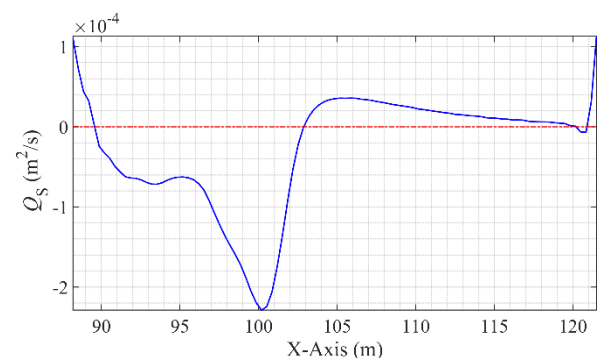


Fig. 4. Averaged surface flow rate (normal) along the swash control plane in the case A6w (sea level = lagoon level) from numerical results.

5 Conclusion

In this paper, a Richards' equation-based model from the *Rivage* code is used to simulate wave-driven beach groundwater flows. Numerical results are compared

against the large-scale BARDEX II experiments. A focus is made on the flow rates through the barrier. The difference between sea and lagoon water levels induces horizontal head gradients which rule the overall barrier groundwater dynamics. Nevertheless, waves generate infiltrations/exfiltrations beneath the swash zone which affect locally the beach saturation and produce vertical flow. These results highlight the establishment of a groundwater circulation cell as swash cycles recur.

Future studies need to evaluate the competition of horizontal and vertical head gradients according to additional parameters (types of waves and beaches) to see the effects on the circulation cell and sediments.

The Czech Technical University in Prague supported this work under the "CTU Global Postdoc Fellowship program".

References

1. D. Sous, L. Petitjean, F. Bouchette, V. Rey, S. Meulé, F. Sabatier, K. Martins, *Adv. Water Resour.* **97**, 144-155 (2016)
2. G. Masselink, A. Rujju, D. Conley, I. Turner, G. Ruessink, A. Matias, C. Thompson, B. Castelle, J. Puleo, V. Citerone, G. Wolters, *Coast. Eng.* **113**, 3-18 (2016)
3. E. Perera, F. Zhu, N. Dodd, R. Briganti, C. Blenkinsopp, I. L. Turner, *Coast. Eng.* **146**, 47-64 (2019)
4. L. Li, D. A. Barry, *Adv. Water Resour.* **23**, 4 (2000)
5. R. Bakhtyar, A. brovelli, D. A. Barry, L. Li, *Coast. Eng.* **58**, 1 (2011)
6. P. Nielsen, *Water Resour. Res.* **26**, 9 (1990)
7. D. Caviedes-Voullième, J. Murillo, P. García-Navarro, *Numerical simulation of groundwater-surface interactions by external coupling of the 3D Richards equation and the full 2D shallow-water equations*, in XIX International Conference on Water Resources (2012)
8. J.-B. Clément, F. Golay, M. Ersoy, D. Sous, *Adv. Water Resour.* **151**, 103897 (2021)
9. M. W. Farthing, F. L. Ogden, *Soil Sci. Soc. Am. J.* **81**, 6 (2017)
10. Y. Mualem, *Water Resour. Res.* **7**, 1 (1971)
11. M. T. van Genuchten, *Soil Sci. Soc. Am. J.* **44**, 5 (1980)
12. M. Zijlema, G. Stelling, P. Smit, *Coast. Eng.* **58**, 10 (2011)
13. B. Rivière, *Discontinuous Galerkin Methods for Solving Elliptic and Parabolic Equations*, SIAM (2008)
14. I. L. Turner, G. C. Rau, M. J. Austin, M. S. Andersen, *Coast. Eng.* **113**, 104-116 (2016)
15. C. H. Benson, I. Chiang, T. Chalermyanont, A. Sawangsuriya, *Estimating van Genuchten Parameters a and n for Clean Sands from Particle Size Distribution Data*, in From Soil Behavior Fundamentals to Innovations in Geotechnical Engineering, ASCE (2014)